

Fermi National Accelerator Laboratory

FERMILAB-Conf-96/218-E

CDF

The CDF Upgrade

C. Newman-Holmes

For the CDF Collaboration

*Fermi National Accelerator Laboratory
P.O. Box 500, Batavia, Illinois 60510*

August 1996

Published Proceedings of the *XI Topical Workshop on ppbar Collider Physics*,
Abano Terme (Padova), Italy, May 27-June 1, 1996

Disclaimer

This report was prepared as an account of work sponsored by an agency of the United States Government. Neither the United States Government nor any agency thereof, nor any of their employees, makes any warranty, expressed or implied, or assumes any legal liability or responsibility for the accuracy, completeness, or usefulness of any information, apparatus, product, or process disclosed, or represents that its use would not infringe privately owned rights. Reference herein to any specific commercial product, process, or service by trade name, trademark, manufacturer, or otherwise, does not necessarily constitute or imply its endorsement, recommendation, or favoring by the United States Government or any agency thereof. The views and opinions of authors expressed herein do not necessarily state or reflect those of the United States Government or any agency thereof.

THE CDF UPGRADE

C. Newman-Holmes
(for the CDF Collaboration)
*Fermilab, P.O. Box 500,
Batavia, IL 60510, USA*

The Collider Detector at Fermilab (CDF) is a general purpose detector used to study the world's highest energy $p\bar{p}$ collisions at the Fermilab Tevatron. Upgrades to CDF to enable it to function as the Tevatron evolves are described.

1 Introduction and Overview

The Collider Detector at Fermilab (CDF) has been used to study $p\bar{p}$ collisions at the Fermilab Tevatron since 1985. Over the years, the Tevatron and CDF have evolved together to yield data sets of increasing sensitivity, from $\sim 0.025 \text{ pb}^{-1}$ in 1987 to $\sim 90 \text{ pb}^{-1}$ in 1994-1996. Fermilab is building a new Main Injector accelerator to further increase the luminosity. This paper describes upgrades to CDF that will enable it to exploit the higher luminosity of the Main Injector. Specifically, the detector must be capable of handling luminosities up to $2 \times 10^{32} \text{ cm}^{-2} \text{ s}^{-1}$ and bunch spacing as small as 132 ns. Several detector systems must be replaced or modified in order to meet these requirements.¹

A cross section of CDF is shown in Figure 1. The detector currently consists of a 1.4 Tesla superconducting solenoid with tracking detectors inside it. Calorimeters (electromagnetic and hadronic) are located outside the magnet and in the forward region. Muon detection is provided by chambers located outside the calorimeters in the central region and by magnetized iron toroid spectrometers in the forward regions. A silicon vertex detector located just outside the beam pipe is used for secondary vertex identification.

The original design of CDF specified a powerful detector with features that have proven to be extremely useful, including excellent calorimetry and tracking capability and a flexible multi-level trigger system. This philosophy is continued with the planned upgrades. The upgrade plans are to:

- Replace the plug and forward gas calorimeters with new scintillator-based calorimeters.
- Replace the Central Tracking Chamber with a new device with shorter drift distance (Central Outer Tracker).
- Replace the silicon vertex detector with a longer double-sided device with faster readout.

The CDF Upgrade

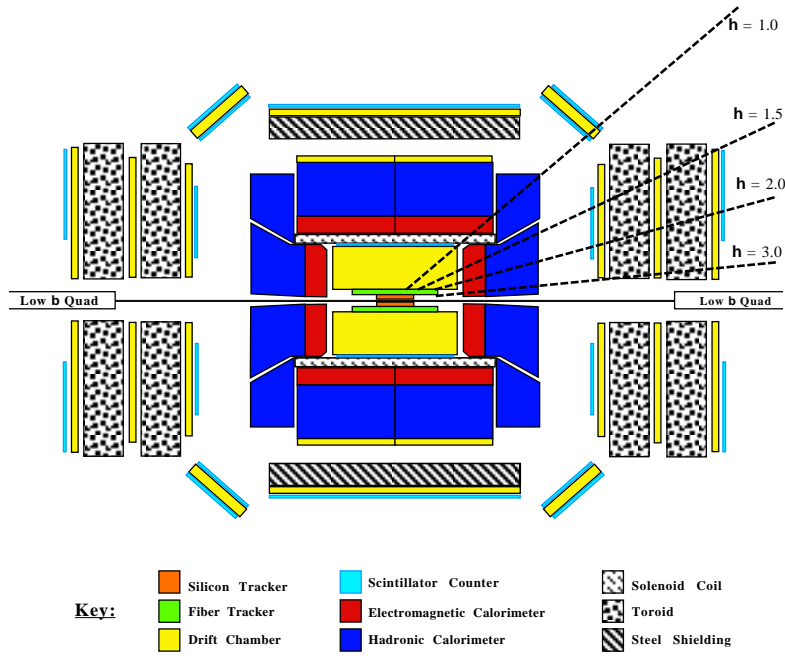


Figure 1: Side view of the upgraded CDF detector.

- Add a new Intermediate Forward Tracker between the silicon vertex detector and the Central Outer Tracker to enhance pattern recognition capability at high luminosities and to provide tracking in the region $1.0 \leq |\eta| \leq 2.0$.
- Upgrade the front-end electronics, trigger and data acquisition systems to accommodate data collection with shorter bunch spacing and higher rates. (Note that the Run I bunch spacing was $3.5 \mu\text{sec}$).

These upgrades are described in more detail below. Additional upgrades to muon detector systems and off-line computing are not discussed here but are described in Ref. 1. Space does not permit a description of the physics capability² of the upgraded CDF. These topics are treated in the references.

Table 1: Design parameters of the baseline tracking systems.

COT	
Radial coverage	48 to 131 cm
Number of superlayers	8
Measurements per superlayer	12
Readout coordinates of SLs	+3° 0 -3° 0 +3° 0 -30°
Maximum drift distance	0.88 cm
Resolution per measurement	180 μ
Rapidity coverage	$ \eta \leq 1.0$
Number of channels	30,240
Material thickness	1.3% X_0
SVXII	
Radial coverage	2.4 to 10.7 cm, staggered quadrants
Number of layers	5
Readout coordinates	r-z, r-z, r- ϕ , r-z, r- ϕ
Readout pitch	60-65 r- ϕ ; 60-150 r-z
Resolution per measurement	12 μ (axial)
Total length	96.0 cm
Rapidity coverage	$ \eta \leq 2.0$
Number of channels	405,504
Material thickness	3.5% X_0
Power dissipated	1.8 KW

2 Tracking Detectors

The upgraded tracking system consists of three parts: a new silicon vertex detector (SVX II), a new Central Outer Tracker (COT) and an Intermediate Forward Tracker (IFT). At this time, the final design for the IFT is under consideration. We discuss the SVX II and COT detectors in this section. A summary of the SVX II and COT design parameters is given in Table 1.

2.1 The Silicon Vertex Detector Upgrade (SVX II)

CDF has had silicon vertex detection capability since 1992. The current silicon detector must be replaced for Run II as the electronics will not work with the shorter bunch spacing. SVX II has the following features:

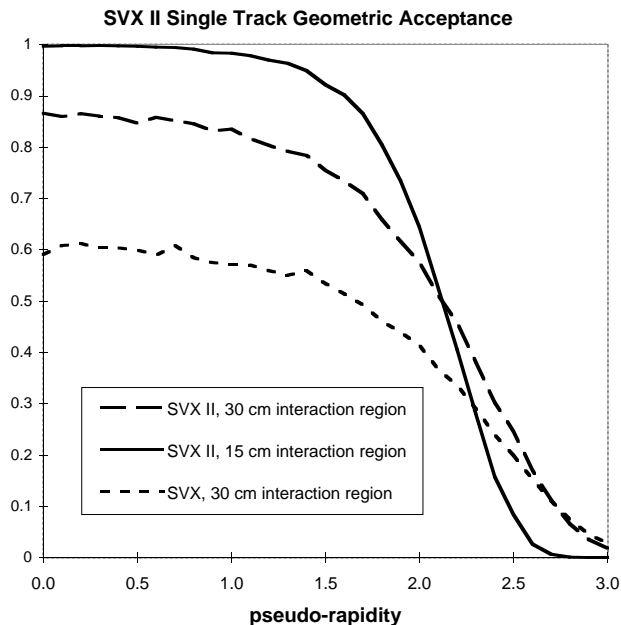


Figure 2: SVX II Track acceptance.

- The barrel (central) region will be longer to cover the luminous region with higher efficiency (see Figure 2).
- The detectors will be double-sided to provide r - z readout for improved pattern recognition and 3-d vertex reconstruction.
- The analog pipeline will be buffered and dual-ported to support simultaneous digitization and readout of data while additional data enter the pipeline ("SVX3" chip). This permits a high Level 1 trigger accept rate (~ 50 kHz) with minimal deadtime.
- Digitization and readout of the SVX II analog data will take approximately 6-7 μ sec following a Level 1 trigger. The high speed of the readout is required in order to use the SVX II data in a Level 2 impact parameter trigger.

The SVX II consists of three barrels, each 32 cm long. There are 12 wedges in ϕ , each with five layers of silicon. Of the five layers, three have 0-90 degree stereo while two have small-angle stereo. For each barrel, the silicon ladders are mounted between two precision-machined beryllium bulkheads.

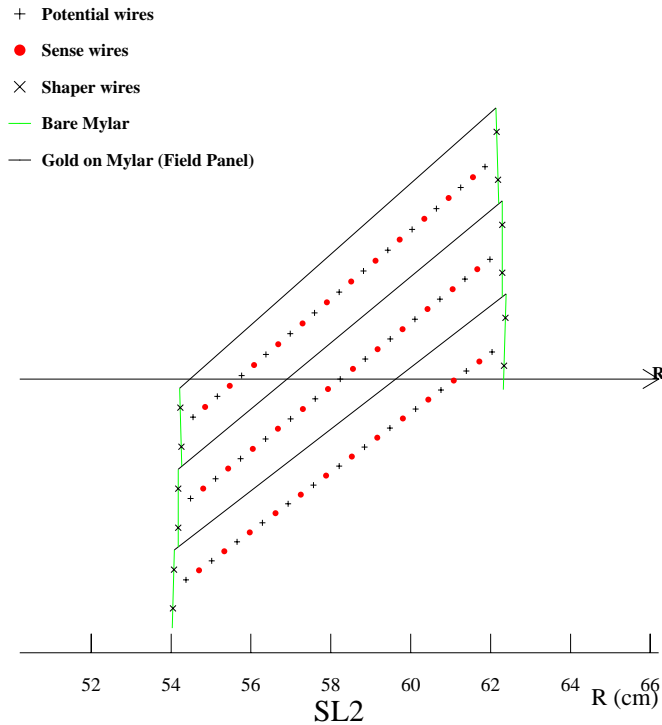


Figure 3: Nominal cell layout for superlayer 2.

2.2 The Central Outer Tracker (COT)

The anchor of the Run II CDF tracking system is a large open cell drift chamber for charged particle reconstruction in the central region $|\eta| \leq 1.0$. This device replaces the Central Tracking Chamber, which would suffer from severe occupancy problems at $\mathcal{L} \geq 1 \times 10^{32} \text{ cm}^{-2} \text{ s}^{-1}$.

The design goal of the COT is to reproduce the functionality of the CTC, but using small drift cells and a fast gas to limit drift times to less than 100 ns. The basic drift cell (Figure 3) will have a line of 12 sense wires alternating with shaper wires every 3.8 mm, running down the middle of two gold-on-mylar cathode planes which are separated by ~ 2 cm. Four axial and four stereo superlayers will provide 96 measurements between 48 and 131 cm, requiring a total of 2,520 drift cells and 30,240 readout channels. The wires and cathode planes are strung between two precision-milled endplates.

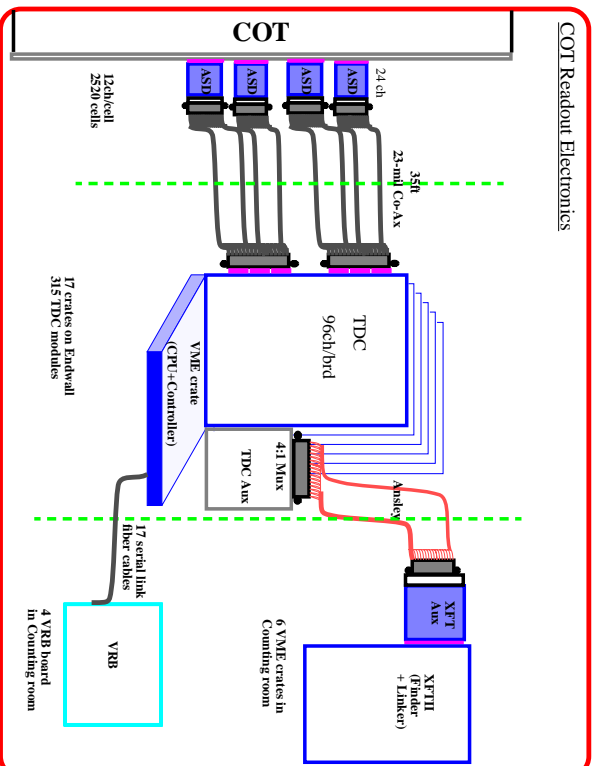


Figure 4: Block diagram for COT readout electronics.

The COT is read out using a pipelined TDC which is standard for CDF wire chamber systems. The tracking information will be available for the Level 1 trigger. A block diagram of the COT electronics is shown in Figure 4.

The COT construction, operation, and offline reconstruction draw heavily on the experience with the CTC, leading to a profound economy in time, expense, and code development. Scaling from the known CTC performance we expect comparable momentum resolution $\delta p_T/p_T^2 = 0.002$, improved track pair separation, and much improved stereo pattern recognition up to luminosities of $2 \times 10^{32} \text{ cm}^{-2} \text{ s}^{-1}$ with 132 ns bunch spacing.

3 Calorimetry

Outside the solenoid, calorimeters (electromagnetic and hadronic) measure particle energies in the region $|\eta| \leq 3.0$. The CDF calorimeters have played a key role in the physics program by measuring electron and photon energies, jet energies, and net transverse energy flow.

For Run II, the central calorimeter of Run I is retained, but in the forward region $|\eta| \geq 1.0$, the gas-based systems are replaced with a new scintillating

Table 2: Central and Plug Upgraded Calorimeter Comparison

	Central	Plug
EM:		
Thickness	$19X_0, 1\lambda$	$21X_0, 1\lambda$
Sample (Pb)	$0.6X_0$	$1X_0$
Sample (scint.)	5 mm	4 mm
WLS	sheet	fiber
Light yield	160 pe/GeV	300 pe/GeV
Sampling res.	$11.6\%/\sqrt{E_T}$	$14\%/\sqrt{E}$
Stoch. res.	$14\%/\sqrt{E_T}$	$16\%/\sqrt{E}$
SM size (cm)	$1.4\phi \times (1.6-2.0)Z$	0.5×0.5 UV
Pre-shower size	$1.4\phi \times 65Z$ cm	by tower
Hadron:		
Thickness	4.5λ	7λ
Sample (Fe)	1 in. C, 2 in. W	2 in.
Sample (scint.)	4 mm	6 mm
WLS	finger	fiber
Light yield	~ 10 pe/GeV	20 pe/GeV

tile plug calorimeter. The new calorimeter consists of an electromagnetic (EM) section followed by a hadronic section. In both sections the active elements are scintillator tiles read out by wavelength shifting (WLS) fibers embedded in the scintillator. The WLS fibers are spliced to clear fibers that carry the light out to photomultiplier tubes (PMT) located on the back plane of each endplug.

The EM calorimeter is a lead/scintillator sampling device with a unit layer composed of 4.5 mm lead and 4 mm scintillator. There are 23 layers in depth for a total thickness of about $21 X_0$ (radiation lengths) at normal incidence. The detecting elements are arranged in a tower geometry pointing back towards the interaction region. The energy resolution of the EM section is approximately $16\%/\sqrt{E}$ with a 1% constant term. The scintillator tiles of the first layer of the EM section are made out of 10 mm thick scintillator and are read out by multi-channel photomultipliers (MCPMTs). They will act as a pre-shower detector. A position detector is located at the depth of the EM shower maximum (approximately $6X_0$). This shower maximum detector is made of scintillator strips read out by WLS fibers; clear fibers carry the light to MCPMTs.

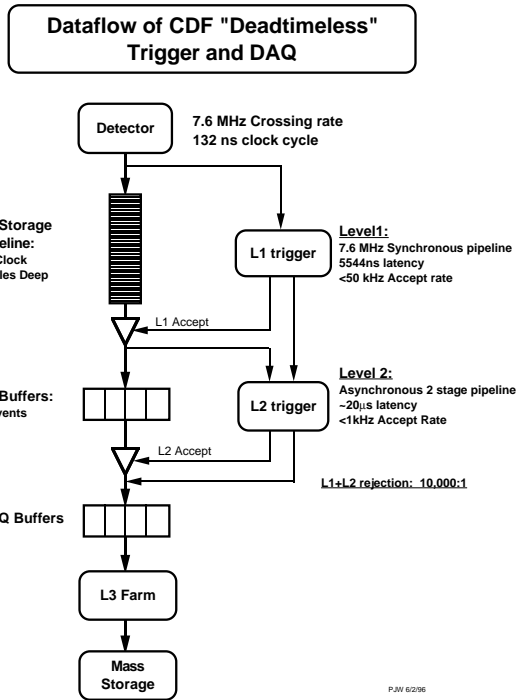


Figure 5: The Run II readout functional block diagram.

The hadron calorimeter is a 23 layer iron and scintillator sampling device with a unit layer composed of 2 inch iron and 6 mm scintillator. The existing iron of the CDF endplugs is used in the new hadron calorimeter: stainless steel disks are attached to the inner 10° cone to extend the coverage to 3° . Two additional stainless steel disks are added behind the electromagnetic section to increase the thickness of the hadron calorimeter. In this way the magnetic field in the tracking volume and the magnetic forces on the end plugs are unchanged. The hadron section has the same tower segmentation as the EM section.

4 Electronics, Trigger and Data Acquisition

The CDF electronics systems must be substantially altered to handle Run II accelerator conditions. The increased instantaneous luminosity requires a similar increase in data transfer rates. However it is the reduced separation between accelerator bunches ($3.5\ \mu\text{sec} \rightarrow 396$ or $132\ \text{ns}$) that has the greatest impact, necessitating a new architecture for the readout system.

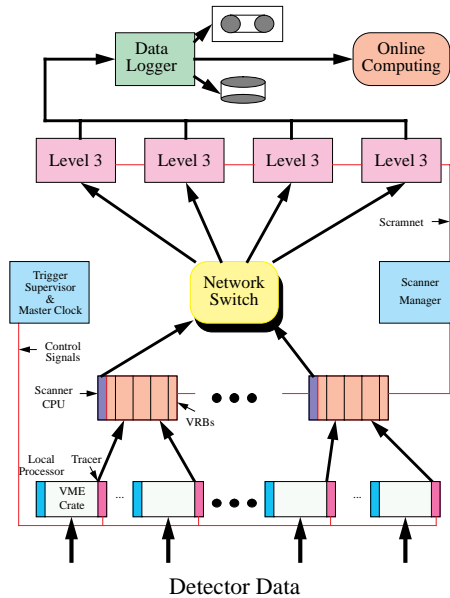


Figure 6: Block diagram of data acquisition system.

Figure 5 shows the functional block diagram of the readout electronics. To accommodate a 132 ns bunch-crossing time and a 4 μsec decision time for the first trigger level, all front-end electronics are fully pipelined, with on-board buffering for 42 beam crossings. Data from the calorimeters, the central tracking chamber, and the muon detectors are sent to the Level 1 trigger system, which determines whether a $\bar{p}p$ collision is sufficiently interesting to hold the data for the Level 2 trigger hardware. The Level 1 trigger is a synchronous system with a decision reaching each front-end card at the end of the 42-crossing pipeline. Upon a Level 1 trigger accept, the data on each front-end card are transferred to one of four local Level 2 buffers. The second trigger level is an asynchronous system with an average decision time of 20 μsec .

A Level 2 trigger accept flags an event for readout. Data are collected in DAQ buffers and then transferred via a network switch to a Level 3 CPU node, where the complete event is assembled, analyzed, and, if accepted, written out to permanent storage. These events can also be viewed by online monitoring programs running on other workstations. A block diagram of the data acquisition system is shown in Figure 6.

With the new system architecture, both the Level 1 and Level 2 accept rates will be an order of magnitude larger than in Run I. For example, with a 40 KHz accept rate from Level 1 and a 300 Hz rate out of Level 2, the system deadtime will be $< 10\%$. The expected rate of events written to mass storage is 30-50 Hz.

5 Conclusions

Upgrades are essential for CDF to function as the Tevatron luminosity increases and the time between collisions decreases. Our upgrade strategy builds on the detector's past successes. We will continue to have excellent tracking with increased redundancy to insure good pattern recognition and momentum resolution as occupancies increase. The calorimetry will be all scintillator-based with resolution equal or better than that of the present detector. The secondary vertex detection capability will be superior to the present detector in acceptance and performance. The electronics, trigger and data acquisition will all operate at much higher rates but with deadtime still kept to a minimum. The CDF upgrade projects will allow us to continue to produce a rich variety of physics results in the Main Injector era.

Acknowledgments

This work was supported by the U.S. Department of Energy and National Science Foundation; the Italian Istituto Nazionale di Fisica Nucleare; the Ministry of Education, Science and Culture of Japan; the National Sciences and Engineering Research Council of Canada; the National Science Council of the Republic of China; and the A.P. Sloan Foundation.

References

1. "The CDF Detector for Tevatron Run II Technical Design Report", by the CDF Collaboration, FERMILAB-PUB in preparation; "The CDF Upgrade", by the CDF Collaboration, CDF note 3171, June, 1995; "Proposal for an Upgraded CDF Detector", by the CDF Collaboration, CDF note 1172, October, 1990.
2. *Future ElectroWeak Physics at the Fermilab Tevatron: Report of the tev_2000 Study Group* Editors D. Amidei and R. Brock Fermilab-Pub-96/082; "Physics with CDF in Run II", by the CDF Collaboration, CDF note 3172, June, 1995. See also talks on future prospects at the Tevatron by A. Byon-Wagner, M. Rijssenbeek, and R. Brock in these Proceedings.